

## Statistical Modelling of Mountain Permafrost Distribution: Local Calibration and Incorporation of Remotely Sensed Data

Stephan Gruber<sup>1,2\*</sup> and Martin Hoelzle<sup>2</sup>

<sup>1</sup>Geographical Institute, Justus Liebig University of Giessen, Germany

<sup>2</sup>Department of Geography, University of Zurich, Switzerland

### ABSTRACT

Field mapping of mountain permafrost is laborious and is generally based on interpolation between point information. A spatial model that is based on elevation and a parameterization of solar radiation during summer is presented here. It allows estimation of permafrost distribution and can be calibrated locally, based on bottom temperature of snow (BTS) measurements or other indicators such as mapped features of permafrost creep. Local calibration makes this approach flexible and allows application in various mountain ranges. Model output consists of a continuous field of simulated BTS values that are subsequently divided into the classes 'permafrost likely', 'permafrost possible' and 'no permafrost' following the rules of thumb established for BTS field measurements in the Alps. Additionally, the simulated BTS values can be interpreted as a crude proxy for ground temperature regime and sensitivity to permafrost degradation. A map of vegetation abundance derived from atmospherically and topographically corrected satellite imagery was incorporated into this model to enhance the accuracy of the prediction. Based on the same corrected satellite image, a map of albedo was derived and used to calculate net short-wave radiation, in an attempt to increase model accuracy. However, the statistical relationship with BTS did not improve. This is probably due to the correlation of short-wave solar radiation with snow-melt patterns or other factors of permafrost distribution which are being influenced differently by the introduction of albedo. Copyright © 2001 John Wiley & Sons, Ltd.

### RÉSUMÉ

La cartographie sur le terrain du pergélisol de montagne est un travail laborieux généralement basé e sur des interpolations entre des points pour lesquelles on possède des informations. Un modèle spatial basé sur l'altitude et le calcul de la radiation solaire est présenté ici. Il permet d'estimer la distribution du pergélisol et peut être calibré localement en utilisant des mesures de température à la base de la neige (BTS) et d'autres indications comme celles résultant de la cartographie des traces de creep du pergélisol. Une calibration locale rend cette approche flexible et permet son application dans différents milieux montagneux. Les données provenant du modèle se présentent comme un champ continu de valeurs BTS simulées qui sont par la suite divisées en classes de "pergélisol probable", "pergélisol possible" et "pergélisol absent" suivant une règle empirique établie pour les mesures BTS dans les Alpes. En outre, les valeurs BTS simulées peuvent être interprétées comme

\*Correspondence to: S. Gruber, Geographical Institute, Justus Liebig University of Giessen, Germany.

Contract/grant sponsor: EU Environment and Climate Research Programme; Contract/grant number: ENV4-CT97-0492.

donnant une approximation du régime de température du sol et de la fragilité à la dégradation du pergélisol.

Une carte de l'abondance de la végétation dérivée d'images satellitaires corrigées pour l'atmosphère et la topographie a été incorporée dans ce modèle dans l'espoir d'augmenter la précision de la prédiction. Basée sur la même image satellitaire corrigée, une carte de l'albedo a été obtenue et utilisée pour calculer la radiation nette dans les ondes courtes pour essayer d'augmenter encore la précision du modèle. Toutefois la relation statistique avec les résultats obtenus par BTS n'a pas été augmentée. Cela est probablement dû à la corrélation existante entre la radiation solaire à courte longueur d'onde et le réseaux de fonte des neiges, ainsi qu'à d'autres facteurs qui contrôlent la distribution du pergélisol en variant différemment de l'albedo. Copyright © 2001 John Wiley & Sons, Ltd.

KEY WORDS: Albedo; GIS; local calibration; remote sensing; statistical permafrost distribution modelling; vegetation abundance

## INTRODUCTION

Permafrost is amongst the most sensitive factors affecting cold-mountain debris-transfer systems with respect to climatic changes (Haeberli, 1996). It plays an important role in the initiation of rock falls, landslides and debris flows as well as other potentially hazardous phenomena. As a consequence, the interest in permafrost research has increased strongly during recent years. The Swiss National Research Project 31 (NFP31) 'Climate Change and Natural Hazard' (Zimmermann *et al.*, 1997; Lugon and Monbaron, 1998; Haeberli *et al.*, 1999) and the European Union project 'Permafrost and Climate in Europe' (PACE) (this issue) reflect this trend and have made valuable contributions to the assessment of environmental and geotechnical hazards associated with permafrost. Numerical permafrost modelling plays an integral part in research and practical application as the only viable means that may be used to estimate these properties spatially.

Direct as well as geophysical or geomorphic evidence of permafrost conditions is generally point information that requires a model for spatial interpolation or extrapolation. In addition, mountain environments pose severe limitations to site access and thus at some locations make numerical modelling the only means for evaluation of geothermal conditions. Temporal extrapolation such as spatial reconstruction and evaluation of past patterns of permafrost distribution, or the incorporation of future climate-change scenarios as projected by global circulation and regional climatic models, are other fields of application for permafrost models. Depending on the task, different modelling approaches may be used (e.g. Keller, 1992; Hoelzle and Haeberli, 1995; Imhof, 1996; Etzelmüller, 1999; Ødegård *et al.*, 1999).

This article presents a statistical model of permafrost distribution that is based mainly on elevation and a parameterization of solar radiation during summer. Furthermore, the incorporation of two remotely sensed parameters is evaluated: a map of vegetation abundance and a map of snow-free albedo used for the calculation of net short-wave radiation. The model can be calibrated locally and its application is therefore not limited to a certain area or mountain range. The modelling strategy introduced here can be implemented using common geographic information systems (GIS) together with standard spreadsheet software.

## STUDY AREA

This study was carried out in the upper Matter Valley (Figure 2), a basin of 485 km<sup>2</sup> surrounding the town of Zermatt. Extensive periglacial areas exist in the area (cf. King, 1990) which has a continental character with high radiation budgets and low precipitation. The glacial equilibrium-line altitude here reaches its highest value in the Alps at approximately 3300 m ASL (Müller *et al.*, 1976; cf. Denneler and Maisch, 1995). Annual average precipitation in the valley ranges from below 600 mm in Grächen to just over 700 mm in Zermatt, both locations being at about 1600 m ASL. Maximum values for the surrounding mountains are estimated as 2000–2500 mm (King, 1996). Most precipitation falls during summer as rain. Zermatt has a mean annual air temperature of +3.7 °C and the local temperature lapse rate is 0.51 °C per 100 m (King, 1996). The timberline is situated at around 2300 m ASL, 400 m higher than in the northern Alps. A high number of active, transitional and relict rock glaciers

in the area are a visible expression of permafrost conditions and their evolution.

## BASIC MODEL DESIGN

Permafrost is a thermal phenomenon that can be described in terms of an energy balance and heat transfer capacity. The most important terms of this energy balance show a strong correlation with permafrost occurrence. Selection of parameters to be included in the model depends on their relative importance, their spatial and temporal variability as well as the effort involved in modelling them with appropriate accuracy. Hoelzle (1994) provides a discussion of the spatio-temporal variability of individual energy balance components. In accordance with the results of that study, elevation and potential incoming short-wave radiation during summer (PSWR) have been chosen as model parameters for this study.

Elevation is mainly a proxy of mean annual air temperature but it should be remembered that it is a compound parameter, in which other correlated phenomena such as the elevation dependence of net long-wave radiation or turbulent fluxes (wind speed) may play an important role. An adequate spatial data field of terrain elevation is provided by the digital elevation model (DEM) of 25 m grid size that was obtained from the Swiss Federal Office of Topography. This 25 m grid formed the common basis on which all other data have been entered and processed in a GIS environment. The PSWR for any pixel is calculated using the Fortran program SRAD (Moore *et al.*, 1993). The program calculates the total incoming solar radiation at every point on a DEM for full days in 12 minute increments. It takes into account the effects of topographic shading, surrounding topography, and different illumination angles for every pixel. Several parameters can be used to tune the model. A circumsolar coefficient (referring to the relative amount of diffuse radiation originating near the solar disk, here set to zero), a cloudiness parameter (radiation fraction reaching the ground during overcast conditions, here set to 1), the sunshine fraction for each month (here set to 1) and ground albedo (here set to 0.15) can be used to tune the model. As potential direct short-wave radiation is the radiation component that exhibits the largest spatial and temporal variability, it was maximized using a sunshine fraction of 1. For application of this permafrost model in more remote areas, this carries the additional benefit of independence from local climate data necessary to estimate realistic radiation parameters. From 15 July until 15 October, daily

potential incoming short-wave radiation has been computed every 30 days. The map of PSWR used for modelling was then derived by averaging of the resulting four daily calculations.

A total of 451 bottom temperature of the winter snow cover (BTS; Haeberli, 1973; Haeberli and Patzelt, 1982; Hoelzle *et al.*, 1993) measurements were available for model design in this study. In spring 1998 and 1999, BTS measurements were carried out in three areas: (1) Trockener Steg/Gandegg, (2) Gornergrat/Stockhorn, (3) Unterrothorn (Figure 2). Positions in the field were determined using a topographic map, a compass, an altimeter and a low-cost GPS receiver. Overlay of downloaded GPS coordinates onto a topographic map in a GIS proved useful, as the spatial pattern of points such as straight lines in a profile could be evaluated and their positions compared with recorded elevations or profile directions. Only a few points were corrected manually for large errors that are most likely due to selective availability of the GPS signal. After correction, the accuracy of most points is believed to be better than one pixel (25 m), but some larger errors of up to 80 m cannot be excluded with certainty, based on the positioning strategy.

For all measured points, attribute values of elevation or PSWR were derived from prepared data layers in a GIS. The histograms in Figure 1 illustrate the character of the measured points. Coverage of important influencing factors such as elevation, slope angle and aspect with BTS points is desirable in order to provide a sound basis for model design. However, existing topography together with little snow cover, difficult access or avalanche danger imposes some restrictions on this aim. Only locations with a snow depth of 80 cm or more were taken into account. The procedure for standardization of BTS measurements to 1 m snow depth as proposed by Haeberli and Epifani (1986) has not been employed in order to avoid additional noise and uncertainties in the model. Positive measured BTS values were considered to be measurement errors and discarded from the dataset. BTS measurements were separated into 371 points used for model design and 80 points for cross-validation, using a random generator.

Based on the 371 'driving' points, a linear multiple regression analysis was performed in order to predict the BTS by using elevation and PSWR as independent variables. The regression yielded a relation of the form:

$$\text{BTS} = a + b \times \text{elevation} + c \times \text{PSWR}$$

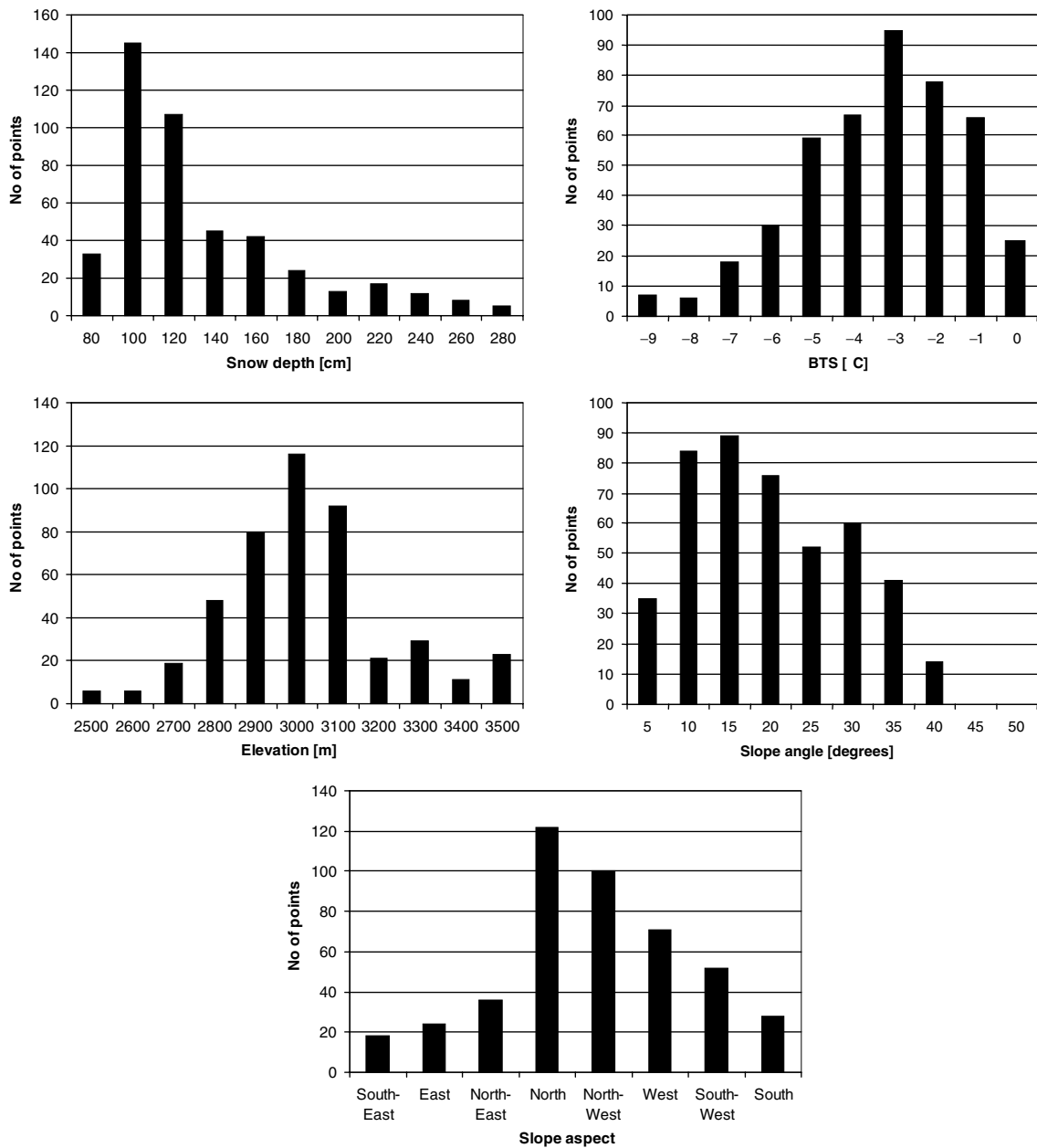


Figure 1 Histograms illustrating the character of the available BTS measurements and their suitability for model calibration.

The coefficients obtained were  $a = 9.913$ ,  $b = -0.0056$  and  $c = 0.113$ , but these should not of course be used in other areas without new analysis. Here 31.2% of the variance is explained by elevation and 7.4% by PSWR, resulting in an overall  $R^2 = 0.386$ . This model was termed MOD1 and applied to the entire project area, generating a continuous

field of simulated BTS. Subsequent slicing into the classes:

- $< -3\text{ }^\circ\text{C}$  likely permafrost (LP)
- $-3\text{ to }-2\text{ }^\circ\text{C}$  possible permafrost (PP)
- $> -2\text{ }^\circ\text{C}$  no permafrost (NP)

in accordance with the standard established for real BTS measurements provided the final model that could be compared visually with rock glaciers and other sites of known permafrost conditions.

## INCORPORATION OF REMOTELY SENSED INFORMATION

### Satellite Imagery Used and its Correction

Summer (snow-free) albedo and vegetation abundance are the two most promising parameters for statistical permafrost modelling that can be acquired in a relatively straightforward way using operational optical orbiting sensors such as Landsat TM. For the derivation of albedo, a larger number of spectral bands are advantageous as this reduces the error inherent in interpolation of wavelength regions not covered by the sensor. Landsat TM was therefore preferred over sensors such as SPOT XS/Xi or IRS-1C LISS-III as it features six reflective bands. In order to benefit from maximum snow-free area and to still have a well-developed plant cover, a cloud-free scene from 12 September 1985 was selected.

Accurate compensation of illumination effects and scatter is crucial for the determination of ground albedo, especially in rugged terrain. A map of vegetation abundance is commonly derived through band ratios and therefore is far less sensitive to illumination differences than the derivation of albedo. Selective scatter and adjacency radiation, however, may still influence this ratio differently, depending on elevation, and as a consequence simple haze removal techniques are not appropriate here. It was therefore necessary to correct the Landsat TM image for topographic and atmospheric effects. This correction has been performed by the German Aerospace Centre (DLR), using a DEM and the program ATCOR3 described in detail by Richter (1998a; 1998b). After correction, images of reflectance were available for all six non-thermal bands. A total of 9.3% of the project area comprises solar illumination angles of  $78^\circ$  or larger during the time of overpass and is thus either in complete shadow ( $>90^\circ$ ), or in cast shadow, or subject to illumination angles that will not yield dependable information, despite correction. In the area of interest, generally no vegetation was present on the very steep north-exposed slopes that were subject to low illumination. Therefore, no interpolation or estimation technique was used to fill these gaps.

### Albedo and Net Short-Wave Radiation

Ground albedo is the ratio of broadband reflected over incident short-wave radiation (in this case  $0.3\text{--}2.5\ \mu\text{m}$ ). For its determination it is necessary to quantify both incoming and reflected radiation. After atmospheric and topographic correction of the satellite image, the resulting reflectance values were integrated and regions between spectral bands interpolated. The algorithm and assumptions used are described in Richter (1998b). The resulting image is a 'snapshot' of summer albedo and does not take into account spatio-temporal variations due to changes in soil moisture or vegetation cover that occur during one season. The availability of an albedo map (cf. Hoelzle, 1994) allowed calculation of the net short-wave radiation:

$$\text{net short-wave radiation} = \text{PSWR} \times (1 - \text{albedo})$$

As this represents the physical reality of energy entering the ground more accurately than the use of just PSWR, it was hoped to enhance model accuracy by incorporation of an albedo map. However, a comparison of PSWR and net short-wave radiation using all 451 BTS measurements indicated a coefficient of correlation with BTS of 0.23 for PSWR and 0.20 for net short-wave radiation. Regression analysis of BTS versus elevation and net short-wave radiation revealed 31.2% of variance explained by elevation and 6.6% by net short-wave radiation. The resulting  $R^2 = 0.378$  is slightly lower than that achieved using PSWR and elevation ( $R^2 = 0.386$ ).

In statistical models, PSWR is probably a compound parameter that owes part of its power to other factors influencing permafrost distribution that are correlated with it. In the attempt to improve the model by introduction of the albedo map, the benefit is probably offset by the effect on the relationship with the remaining correlated factors. The snow-free duration of a site is likely to be such a factor. Sites with high amounts of PSWR will (at the same altitude) generally become snow-free earlier and thus have more solar irradiation contributing to their annual ground heat flux. The snow-free duration of a site will not be influenced by summer albedo and therefore correlates less with net short-wave radiation than with PSWR. It may, however, be an equally important parameter. It was therefore decided not to use the albedo map, as this might introduce an additional source of error into the model without enhancing its statistical basis. This result demonstrates the 'grey-box' character of

this modelling approach which is based on physical processes but does not resolve individual energy balance terms or feedback mechanisms.

### Vegetation Abundance

Vegetation is an important indicator of permafrost distribution (e.g. Haeberli, 1975; Hoelzle, 1994; Frauenfelder *et al.*, 1998) and, for its incorporation into spatial models, quantitative, coherent information on vegetation cover is necessary. The instantaneous acquisition of multi-spectral data makes satellite imagery useful for studies of plant cover density. A wealth of indices exists to parameterize the amount of green vegetation. They are mostly based on the steep slope between 0.68 and 0.76  $\mu\text{m}$  in vegetation reflectance spectra, which is commonly called the 'red edge'. The soil-adjusted vegetation index (SAVI) proposed by Huete (1988) was chosen to parameterize vegetation abundance in the project area, comprising strong lateral variability of soil properties and moisture contents. It should, however, be kept in mind that research and development of vegetation indices was mostly aimed at agricultural applications and that employing these methods in high mountains remains somewhat experimental. As vegetation abundance in the areas of interest approaches zero, the signal-to-noise ratio becomes highly unfavourable.

The matrix of correlation coefficients in Table 1 shows a good correlation of SAVI with BTS but also a high inter-correlation of SAVI with elevation as well as with PSWR, which makes regression analysis less robust. Having in mind the additional error inherent in the SAVI map and its inter-correlation with other independent variables, the contribution of this parameter to a model of permafrost distribution needs to be evaluated carefully.

Table 1 Coefficients of correlation between parameters used for regression analysis and measured BTS values. Elevation and PSWR exhibit a low inter-correlation whereas the vegetation abundance represented by SAVI correlates strongly with both other parameters.

	BTS	Elevation	PSWR
Elevation	-0.54		
PSWR	0.23	0.05	
SAVI	0.45	-0.56	0.21

A multiple linear regression was performed based on elevation, PSWR in summer and SAVI in order to predict BTS, using the same 371 data points as in the case of MOD1. The regression yielded a relation that can be used for subsequent modelling:

$$\text{BTS} = a + b \times \text{elevation} + c \times \text{PSWR} + d \times \text{SAVI}$$

The coefficients obtained were  $a = 7.809$ ,  $b = -0.0048$ ,  $c = 0.102$  and  $d = 4.933$ , but these should not be used in other areas without new analysis. A total of 31.2% of the variance is explained by elevation, 7.4% by PSWR and 1.2% by SAVI, resulting in an overall  $R^2 = 0.398$ . The resulting simulation of BTS temperatures over the entire project area was termed MOD2 and sliced into the three classes of permafrost distribution defined above.

### EVALUATION AND VALIDATION OF MODELS

The BTS is a proxy of ground temperature regime and thus permafrost distribution. The correlation between BTS and ground temperature regime itself is not high and sometimes measurements show a high variation within short distance. Local effects such as snow depth, snow cover evolution, the quality of the contact between ground surface and the temperature probe, circulation of cold air in vents etc. can greatly influence individual BTS measurements (cf. Keller and Gubler, 1993; Bernhard *et al.*, 1998; Ikeda, 2000). These local effects are assumed to be non-systematic and expected to be smoothed out partly by the high number of measurements used in the regression. The modelled values of 'potential BTS' should therefore give a good general estimation of permafrost conditions.

Of the BTS measurements, 80 were not used in the regression analysis for model construction but were kept aside for cross-validation. Table 2 gives an overview of the success in predicting the three classes of permafrost distribution. The agreement between the models and the measured BTS as expressed by Kendall's  $\tau$  is 0.33 for MOD1 and 0.40 for MOD2, where  $\tau = 1$  would indicate perfect agreement and  $\tau = 0$  no agreement or random classification.

For MOD1, 46 of 80 points were correctly assigned to the three classes; all others except for 8 points were assigned to a neighbouring class. Of 27 points assigned to a neighbouring class, 17 were estimated in favour of permafrost. For MOD2, 47 of 80 points were correctly assigned to the three classes; all others

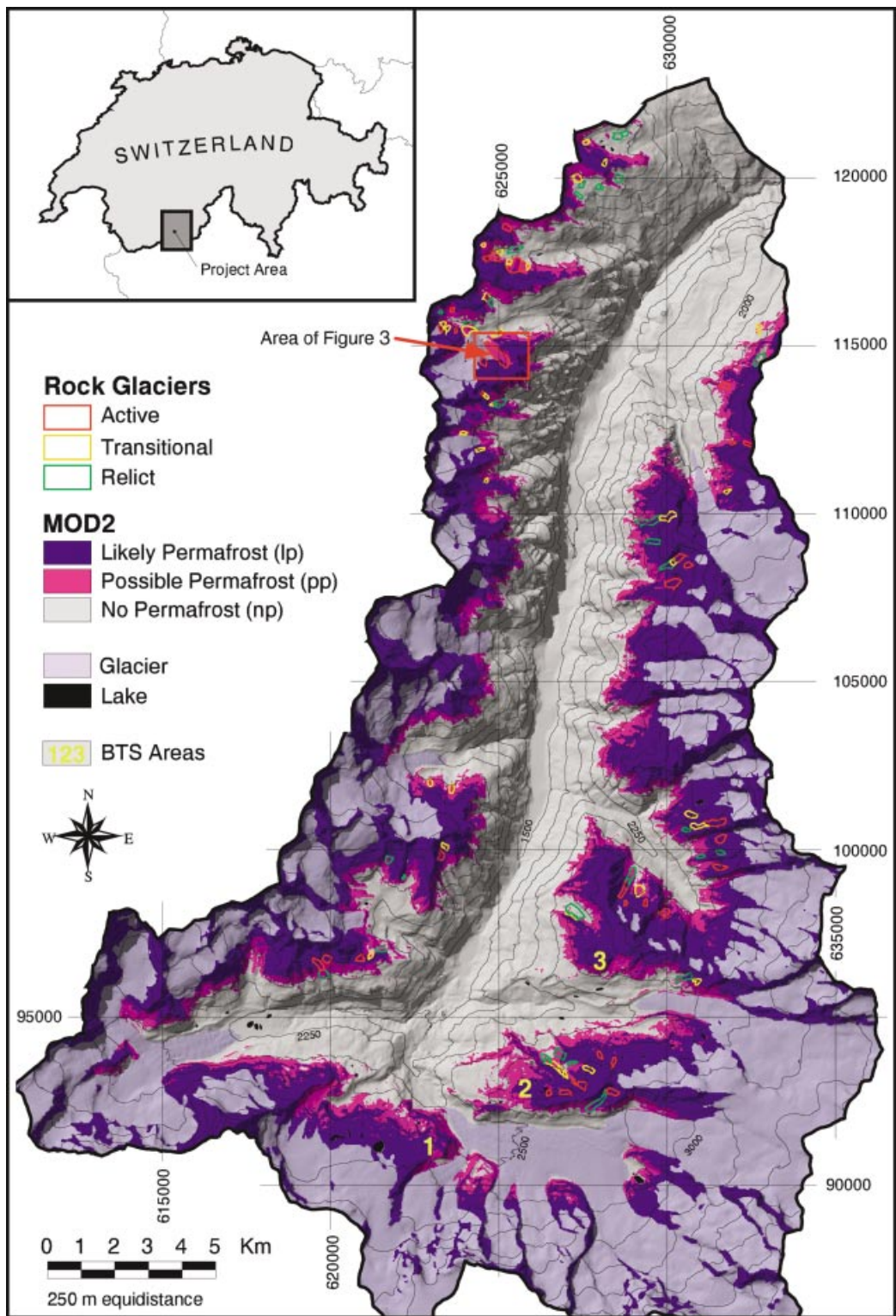


Plate 1 Distribution of modelled permafrost, rock glaciers and glaciers for the project area Matter Valley.

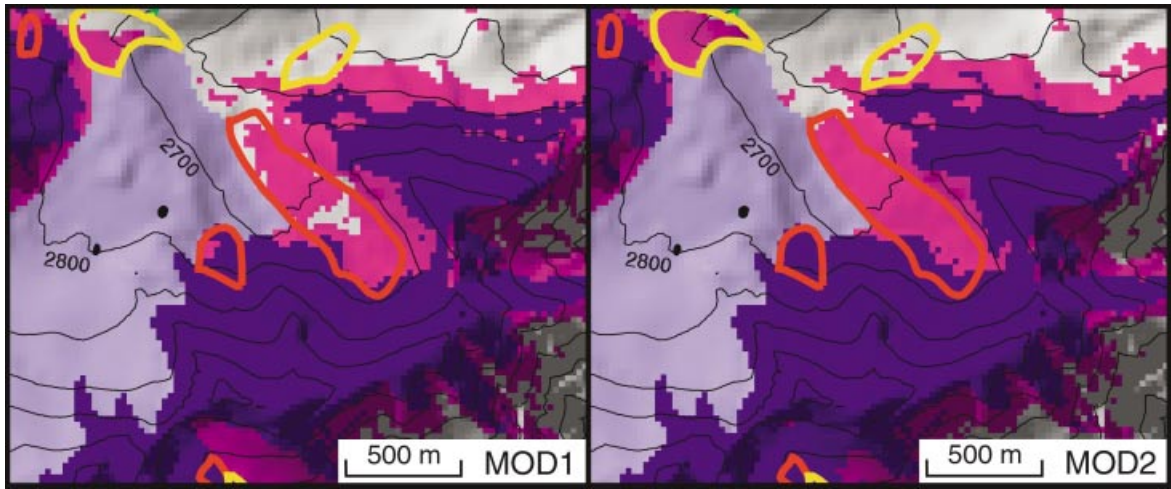


Plate 2 Visual comparison of the model with (MOD2) and without (MOD1) incorporation of vegetation abundance. MOD2 depicts the extent of the large active rock glacier more accurately. See Plate 1 for key.

Table 2 Results of cross-validation performed on the model with incorporation of vegetation abundance (MOD2) and without (MOD1). LP refers to 'likely permafrost', PP to 'possible permafrost' and NP to 'no permafrost' based on model predictions compared with measured BTS values.

BTS	MOD1			Total	BTS	MOD2			Total
	LP	PP	NP			LP	PP	NP	
LP	<b>40</b>	9	1	50	LP	<b>42</b>	7	1	50
PP	8	<b>4</b>	0	12	PP	9	<b>2</b>	1	12
NP	7	9	<b>2</b>	18	NP	6	9	<b>3</b>	18
Total	55	22	3	46	Total	57	18	5	47

except for 7 points were assigned to a neighbouring class. Of 26 points assigned to a neighbouring class, 18 were estimated in favour of permafrost. The cross-validation shows MOD2 to provide a slightly better estimate of permafrost distribution than MOD1, in accordance with the slightly larger  $R^2$  of MOD2. However, this small gain might not be counterbalanced by the unfavourable signal-to-noise ratio and the inter-correlating regressor variables that can be expected in the SAVI map.

Therefore a further, visual assessment was performed in a GIS. This was based on field knowledge of permafrost occurrence and provided an insight into the modelled spatial permafrost distribution in this well-researched area. Plate 1 shows an overview of the project area and the permafrost distribution calculated by MOD2. A total of 103 rock glaciers, which provide a good indicator of model accuracy, are shown. They were mapped from black and white aerial photographs and tentatively assigned to three classes of activity. Of these rock glaciers, 20, including those depicted in Plate 2, were visited in summer 1999 and their activity described in the field. Details of the mapping process as well as the criteria used to judge the activity status of rock glaciers, are outlined in Gruber (2000).

The better agreement of MOD2 with the rock glacier outline (the red, diagonal feature) can be seen in Plate 2. In terms of approximating the energy balance at the surface, the result of MOD1 is not necessarily wrong, as creeping permafrost protected by a coarse blocky layer can move beyond the zone of active permafrost. However, studies in other areas in Switzerland (e.g. Gornergrat/Riffelhorn and north of Gornergrat) have demonstrated the value of using SAVI as a model parameter to resolve some local variations due to unvegetated, coarse blocky surfaces or the indicator value of dense vegetation. This fact, together with the slightly higher

$R^2$  and Kendall's  $\tau$  of MOD2, supports the conclusion that the introduction of vegetation abundance can enhance the performance of statistical models despite the statistically less robust design due to inter-correlation of the independent variables. It should be kept in mind that the indicator value that vegetation has for permafrost distribution varies considerably between different mountain ranges and climatic conditions.

## CONCLUSIONS AND OUTLOOK

A permafrost modelling strategy based on potential incoming short-wave radiation during summer (PSWR) and terrain elevation that allows for local calibration is outlined. Local calibration makes this method flexible and opens the possibility that this model may be used in other areas where climatic characteristics are different. This approach is currently in progress in the Corral del Veleta in the Spanish Sierra Nevada. A further experiment showed that BTS values roughly estimated from mapped rock glaciers could be successfully used for model design in the Swiss study area. The proposed modelling strategy can be implemented using a wide range of easily available software packages and is therefore open to a wide community. The program SRAD that is used for calculation of solar radiation is freely available on the Internet for research purposes. Considerable skill and experience are, however, necessary for the acquisition of data needed to set up and evaluate the model. As the model described here simulates a continuous field of BTS values, it can be divided into different numbers of permafrost distribution classes according to the task at hand. Furthermore, a crude proxy of ground temperature regime and therefore the sensitivity of permafrost to disturbances is inherent in such a continuous score of 'permafrost potential'.

Vegetation abundance was parameterized based on Landsat TM imagery and incorporated into the spatial permafrost model. The satellite imagery used had been atmospherically and topographically corrected; however, in the case of a vegetation index, this is most likely not crucial for practical application. Although subject to an unfavourable signal-to-noise ratio and inter-correlation with elevation and PSWR, vegetation abundance was shown to be a potentially valuable model parameter.

Incorporating a map of summer albedo into a radiation-based statistical model proved fruitless, however, despite the fact that the use of net short-wave radiation instead of just PSWR more closely resembles energy entering the ground from solar irradiation. This demonstrates that statistical modelling

such as this gives only an approximate estimate of the actual processes involved in the energy balance. Recent research that focuses on representation of physical processes by measuring and modelling individual terms of the energy balance over Alpine permafrost (Mittaz, 1998; Mittaz *et al.*, 2000; Imhof *et al.*, 2000) will contribute substantially to further process understanding. Application of such process models will be restricted to individual areas where precise information is available. However, the insight gained as well as the output of process models will provide a novel basis for calibration and refinement of more simple statistical models that demand less data input and that are computationally less intense.

## ACKNOWLEDGEMENTS

Rudolf Richter from the Institute of Optoelectronics at the German Aerospace Centre (DLR) performed the atmospheric and topographic correction of the satellite scene used in this study. Lorenz King supervised the MSc thesis on which this study is based. The data used have been funded through the European Union PACE project (ENV4-CT97-0492) coordinated by C. Harris, University of Cardiff, UK. Thanks are due to Wilfried Haerberli and Monika Gruber for carefully reading the manuscript.

## REFERENCES

- Bernhard L, Sutter F, Haerberli W, Keller F. 1998. Processes of snow/permafrost interactions at a high-mountain site, Murtel/Corvatsch, Eastern Swiss Alps. In *Proceedings of the 7th International Conference on Permafrost, Yellowknife, Canada, 1998*. Nordicana, 57, 35–41.
- Denneler B, Maisch M. 1995. Gletscher und Gletscherschwund im Mattertal (Südliche Walliser Alpen, VS). *Bull. Murithienne* **113**: 147–171.
- Etzelmüller B, Berthling I, Sollid JL. 1998. The distribution of permafrost in southern Norway—a GIS approach. In *Proceedings of the 7th International Conference on Permafrost, Yellowknife, Canada, 1998*. Nordicana, 57, 251–257.
- Frauenfelder R, Allgoewer B, Haerberli W, Hoelzle M. 1998. Permafrost investigations with GIS—a case study in the Fletschhorn area, Wallis, Swiss Alps. In *Proceedings of the 7th International Conference on Permafrost, Yellowknife, Canada, 1998*. Nordicana, 57, 291–295.
- Gruber S. 2000. Slope instability and permafrost—a spatial analysis in the Matter Valley, Switzerland. Master's thesis, Justus Liebig University, Giessen, Germany.
- Haerberli W. 1973. Die Basistemperatur der winterlichen Schneedecke als möglicher Indikator für die Verbreitung von Permafrost in den Alpen. *Zeitschrift für Gletscherkunde und Glazialgeologie* **XI**(1–2): 221–227.
- Haerberli W. 1975. *Untersuchungen zur Verbreitung von Permafrost zwischen Flüelapass und Piz Grialetsch (Graubünden)*. Mitteilungen der Versuchsanstalt für Wasserbau, Hydrologie und Glaziologie, ETH Zürich, 17.
- Haerberli W. 1992. Construction, environmental problems and natural hazards in periglacial mountain belts. *Permafrost and Periglacial Processes* **3**: 111–124.
- Haerberli W. 1996. On the morphodynamics of ice/debris-transport systems in cold mountain areas. *Norsk geografisk Tidsskrift* **50**: 3–9.
- Haerberli W, Epifani F. 1986. Mapping the distribution of buried glacier ice—an example from Lago Delle Locce, Monte Rosa, Italian Alps. *Annals of Glaciology* **8**: 78–81.
- Haerberli W, Patzelt G. 1982. Permafrostkartierung im Gebiet der Hochebenkar-Blockgletscher, Obergurgl, Ötztaler Alpen. *Zeitschrift für Gletscherkunde und Glazialgeologie* **17**: 127–150.
- Haerberli W, Hoelzle M, Boesch H, Funk M, Kaeab A, Vonder Muehll D, Keller F. 1999. *Eisschwund und Naturkatastrophen im Hochgebirge*. Schlussbericht NFP31, vdf/ETHZ.
- Hoelzle M. 1994. *Permafrost und Gletscher im Oberengadin. Grundlagen und Anwendungsbeispiele für automatisierte Schätzverfahren*. Mitteilungen der Versuchsanstalt für Wasserbau, Hydrologie und Glaziologie, ETH Zürich, 132.
- Hoelzle M, Haerberli W. 1995. Simulating the effects of mean annual air temperature changes on permafrost distribution and glacier size: an example from the Upper Engadin, Swiss Alps. *Annals of Glaciology* **21**: 399–405.
- Hoelzle M, Haerberli W, Keller F. 1993. Application of BTS measurements for modelling mountain permafrost distribution. In *Proceedings of the Sixth International Conference on Permafrost, Beijing*. vol. 1, 272–277.
- Huete AR. 1988. A soil-adjusted vegetation index. *Remote Sensing of Environment* **25**: 295–309.
- Ikeda A. 2000. Rock glacier morphology, structure and processes in the Upper Engadin, Swiss Alps: the effect of rock types and thermal conditions. PhD thesis, University of Tsukuba, Japan.
- Imhof M. 1996. Modelling and verification of the permafrost distribution in the Bernese Alps (Western Switzerland). *Permafrost and Periglacial Processes* **7**: 267–280.
- Imhof M, Pierrehumbert G, Haerberli W, Kienholz H. 2000. Permafrost investigations in the Schilthorn Massif (Bernese Alps, Switzerland). *Permafrost and Periglacial Processes* **11**: 189–206.
- Keller F. 1992. Automated mapping of mountain permafrost using the program PERMAKART within the geographical information system ARC/INFO. *Permafrost and Periglacial Processes* **3**: 133–138.

- Keller F, Gubler HU. 1993. Interaction between snow cover and high-mountain permafrost, Murtel/Corvatsch, Swiss Alps. In *Proceedings of the Sixth International Conference on Permafrost, Beijing*. vol. 1, 332–337.
- King L. 1990. Soil and rock temperatures in discontinuous permafrost: Gornergrat and Unterrothorn, Wallis, Swiss Alps. *Permafrost and Periglacial Processes* **1**: 177–188.
- King L. 1996. Dauerfrostboden im Gebiet Zermatt—Gornergrat—Stockhorn: Verbreitung und permafrostbezogene Erschließungsarbeiten. *Zeitschrift für Geomorphologie NF, Suppl.-Bd.* **104**: 73–93.
- Lugon R, Monbaron M. 1998. *Stabilité des terrains meubles en zone de pergélisol et changements climatiques*. Schlussbericht NFP31, vdf/ETHZ.
- Mittaz C. 1998. Energiebilanz ueber Alpinem Permafrost. In *Mitteilungen der Versuchsanstalt für Wasserbau, Hydrologie und Glaziologie, ETH Zürich*, 158, 152–167.
- Mittaz C, Hoelzle M, Haeberli W. 2000. First results and interpretation of energy flux measurements over Alpine permafrost. *Annals of Glaciology*, **31**: 427–433.
- Moore ID, Norton TW, Williams JE. 1993. Modelling environmental heterogeneity in forested landscapes. *Journal of Hydrology* **150**: 717–747.
- Müller F, Caffisch T, Müller G. 1976. *Firn und Eis der Schweizer Alpen. Gletscherinventar*. Geographical Institute of the ETH Zürich, 57.
- Ødegård RS, Isaksen K, Mastervik M, Billdal L, Engler M, Sollid JL. 1999. Comparison of BTS and Landsat TM data from Jotunheimen, southern Norway. *Norsk geografisk Tidsskrift* **53**: 226–233.
- Richter R. 1998a. Correction of satellite imagery over mountainous terrain. *Applied Optics* **37**: 4004–4015.
- Richter R. 1998b. Value adding products derived from the ATCOR models. Unpublished internal report at DLR, German Aerospace Center, Institute for Optoelectronics.
- Zimmermann M, Mani P, Gamma P, Gsteiger P, Hunziker G, Heiniger O. 1997. *Beurteilung der Murganggefahr mit Hilfe eines Geographischen Informationssysteme. Analyse der räumlichen Entwicklung infolge von Klimaänderungen*. Schlussbericht NFP31, vdf/ETHZ.